THE JOURNAL OF PHYSICAL CHEMISTRY C

Article

pubs.acs.org/JPCC

Energy Landscape of Water and Ethanol on Silica Surfaces

Di Wu,[†] Xiaofeng Guo,[†,‡] Hui Sun,[§] and Alexandra Navrotsky*[,†]

[†]Peter A. Rock Thermochemistry Laboratory and NEAT ORU, University of California, Davis, One Shields Avenue, Davis, California 95616, United States

[‡]Earth System Observations, Earth and Environmental Sciences Division, Los Alamos National Laboratory, Los Alamos, New Mexico 87545, United States

[§]State Key Laboratory of Chemical Engineering, East China University of Science and Technology, Shanghai 200237, China

ABSTRACT: Fundamental understanding of small molecule−silica surface interactions at their interfaces is essential for the scientific, technological, and medical communities. We report direct enthalpy of adsorption (Δh_{ads}) measurements for ethanol and water vapor on porous silica glass (CPG-10), in both hydroxylated and dehydroxylated (hydrophobic) forms. The results suggest a spectrum of energetics as a function of coverage, stepwise for ethanol but continuous for water. The zero-coverage enthalpy of adsorption for hydroxylated silica shows the most exothermic enthalpies for both water (−72.7 ± 3.1 kJ/mol water) and ethanol (−78.0 ± 1.9 kJ/mol ethanol). The water adsorption enthalpy becomes less exothermic gradually until reaching its only plateau (−20.7 ± 2.2 kJ/mol water) reflecting water clustering on a largely hydrophobic surface, while the enthalpy of ethanol adsorption profile presents two well separated plateaus, corresponding to strong chemisorption of ethanol on adsorbate-free silica surface (−66.4 ± 4.8 kJ/mol ethanol), and weak physisorption of ethanol on ethanol covered silica (−4.0 ± 1.6 kJ/mol ethanol). On the other hand, dehydroxylation leads to missing water−silica interactions, whereas the number of ethanol binding sites is not impacted. The isotherms and partial molar properties of adsorption suggest that water may only bind strongly onto the silanols (which are a minor species on silica glass), whereas ethanol can interact strongly with both silanols and the hydrophobic areas of the silica surface.

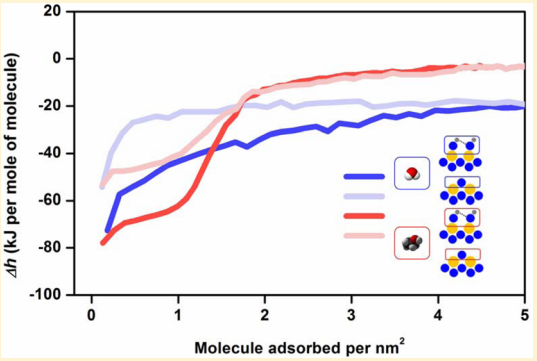

INTRODUCTION

Silica forms the basis for one of the most abundant and complex groups of inorganic structures, existing in the natural environment as minerals[1] and being produced synthetically as industrial materials.[2,3] Its various polymorphs may interact with small organic molecules and water, and are extensively applied in many scientific and technological fields, ranging from classic heterogeneous catalysis[4−7] to recently developed organo-silica hybrid nanodevices.[8,9] Organics encapsulated in silica nanoparticles are also employed to assist medical diagnoses and treatments,[10] such as tumor targeted drug delivery.[11,12] In all such applications, the energetics of adsorbate−surface binding is critical to function. On a larger scale, the thermodynamics of such interactions may also influence reactions at small molecule−mineral interfaces encountered under geological conditions, including in oil and natural gas recovery and CO_2 sequestration.[13−18] Despite the variety and complexity of organic−silica interactions, they seem to be largely governed by hydrophobicity/hydrophilicity and/or acidity/basicity.[19,20] Numerous studies were performed on the structure of silica polymorphs[21−25] and kinetics of surface binding.[26,27] However, a systematic thermodynamic study of organic−silica interactions as functions of molecular coverage and surface hydrophobicity has not been reported. Nor has there been much direct comparison of the energetics of interaction of a given form of silica with water versus with simple organic molecules. Such differences in energetics form the basis for the competitive binding of water and organics to that surface, which in turn defines chemical, catalytic, biological, environmental, and geological reactivity.

We previously performed a series of studies on organic−silica interactions using aqueous solution and solvent immersion calorimetry.[28−31] Here, we take a different approach. Direct gas adsorption calorimetry,[32] is employed to investigate the energetics of small organic molecule−silica binding. The experimental setup includes an accurate gas dosing system coupled with a Calvet twin microcalorimeter,[32] which enables precise and simultaneous monitoring of the adsorption isotherm and associated heat effect for each small dose of adsorbing gas. Our initial water adsorption calorimetry studies revealed complex energetics as a function of molecular coverage for nanoparticle surface hydration and suggested heterogeneous yet continuously distributed energetics of surface binding sites.[32−40] Later, we extended gas adsorption calorimetry to study CO_2 capture sorbents,[41,42] in which stepwise energetics corresponding to binding on different functional groups were revealed. Most recently, we expanded the experimental

Received: May 4, 2015
Published: June 12, 2015

DOI: 10.1021/acs.jpcc.5b04271
J. Phys. Chem. C 2015, 119, 15428−15433

capability by using pure ethanol as the vapor source and studied its interaction with calcite nanoparticles. We revealed a complex energetic landscape, more complicated than that of the water−nanocalcite system.[43] The existence of a region of low ethanol density between the first and second layer of adsorbed ethanol, suggested by molecular dynamics and spectroscopy,[43−45] was strongly supported by our calorimetric data by showing a near zero differential adsorption enthalpy for ethanol molecules adsorbed after formation of the monolayer. These data strongly suggested discontinuous configuration of ethanol but continuity for water layers on nanocalcite.

In the present work, we study the adsorption enthalpies of water and ethanol vapor on porous silica glass with both hydroxylated and hydrophobic surfaces. Our major goal is to understand the energetics of water and small organics on silica surface as functions of molecular coverage and hydrophobicity. Ethanol is selected to represent a small polar organic adsorbate, while water adsorption is performed for comparison. Controlled pore glass CPG-10, a synthetic, mesoporous silica with uniform surface and structural chemical properties is the adsorbent. The advantage of this particular silica material is that one can manipulate the degree of hydrophobicity by tailoring the number of hydroxyls through thermal treatment. Specifically, the adsorbed water molecules can be removed at 200 °C, releasing free hydroxyls (silanols). Further heating leads to dehydroxylation at 800 °C, resulting in a purely hydrophobic silica surface with only Si—O—Si bonds (siloxanes, see Figure 1a).[46] We believe water and ethanol adsorption calorimetric measurements on both hydroxylated and dehydroxylated (hydrophobic) silica surfaces in a controlled manner will enhance our understanding of small molecule−silica interactions.

EXPERIMENTAL SECTIONS

Controlled pore silica glass (Millipore, CPG75C, Lot No. 01C009) was used as representative silica material (see Table 1 for its properties as provided by the manufacturer). Powder X-ray diffraction (XRD) diffraction was performed at room temperature on a Bruker AXS D8 Advance X-ray diffractometer (Cu Kα radiation, 40 kV, 40 mA, 5 to 90° 2θ with a step size of 0.02°at 1 s/step). A full nitrogen adsorption/desorption isotherm was measured at −196 °C using a Micromeritics ASAP 2020 instrument. Prior the isotherm measurement, the sample was degassed at 200 °C to remove any adsorbed species. The Brunauer−Emmett−Teller (BET) equation[47] was applied to obtain specific surface area.

Temperature-programmed desorption mass spectrometry (TPD-MS) was performed using a Netzsch STA 449 coupled with a Micromeritics Cirrus 2 quadrupole mass spectrometry to reveal the distribution of surface water species. About 20 mg of sample was placed in a platinum crucible and heated from 30 to 950 °C at 10 °C/min in argon flow (40 mL/min). The evolved gas was introduced into the ionization chamber of mass spectrometer. The TG and MS signals (H_2O, m/z = 18) were corrected using the reference baselines collected by performing runs without sample under the same experimental conditions.

The water/ethanol adsorption system includes a Calvet-type microcalorimeter (Setaram Sensys), which is coupled to a gas adsorption analyzer (Micromeritics ASAP 2020). About 100 mg of sample was placed into one side of a custom designed silica forked tube, the other side of which was kept empty as a reference. Then the tube was inserted into the twin chambers of the calorimeter and connected to the analysis port of the gas adsorption analyzer. The sample was subjected to degas at elevated temperature under vacuum (<10^{-3} Pa) overnight (12 h) to remove any adsorbed species. Two heating temperature, 200 and 800 °C, were used to achieve silica surfaces with different degrees of hydrophobicity. The degassed samples were labeled S200C and S800C. The water and ethanol adsorption calorimetry was carried out at 25 °C. The ASAP 2020 was programmed in incremental dosing mode (2 μmol per dose) with 1 h equilibration time between doses. The amount of gas adsorbed was measured from the pressure drop at equilibrium. Adsorption of each gas dose resulted in a distinct enthalpy peak. The differential enthalpy of adsorption was calculated using the integrated area of these peaks divided by the amount of adsorbed gas molecules (mole) from each dose. The total surface area of sample analyzed is much more than that of the forked tube, therefore, the trace amount of water adsorbed onto the tube was negligible and did not introduce significant error.

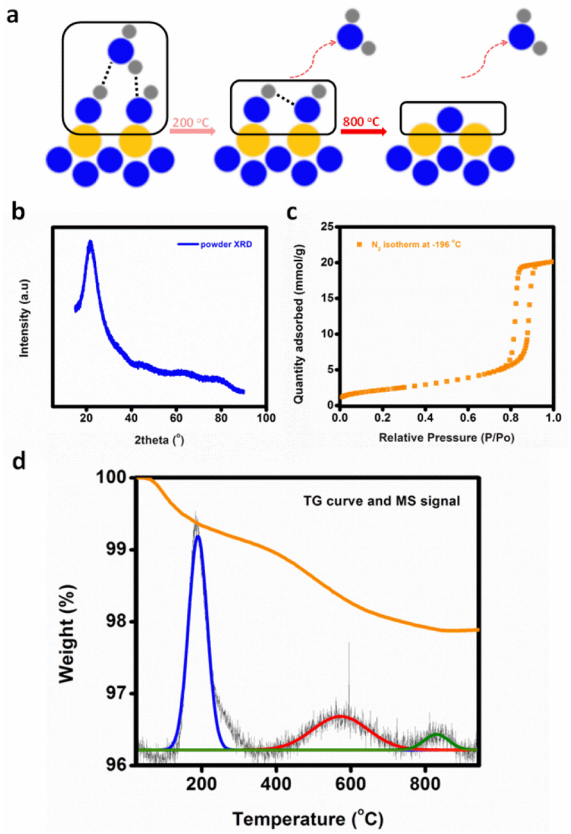

Figure 1. (a) Schematics for dehydration process of silica surface. Gray, blue, and orange spheres denote H, O, and Si atoms, respectively. (b) X-ray diffraction pattern. (c) Nitrogen adsorption isotherm (at −196 °C) of the CPG-10 silica glass and (d) temperature-programmed desorption mass spectrometry (TPD-MS) profile of CPG-10 silica dehydration until 950 °C in flowing argon (40 cc/min).

RESULTS

The powder XRD pattern (Figure 1b) is typical for glassy (amorphous) silica. The nitrogen adsorption/desorption isotherm (Figure 1c) is type IV, featuring narrow, sharply rising hysteresis. This profile supports that the sample has high surface area, uniform nanopores, and narrow pore size distribution (see Table 1).

DOI: 10.1021/acs.jpcc.5b04271
J. Phys. Chem. C 2015, 119, 15428−15433

Table 1. Material Properties of CPG-10 Silica

	specific surface area (m^2/g)	pore diameter (nm)	pore size distribution (±%)	pore volume (cm^3/g)
millipore	197	8.1	8.9	0.49
this study	192	7.8	8.6	0.48

The TPD-MS curve is plotted in Figure 1d. Peak deconvolution was performed using Gaussian multipeak fitting, in which the signal for water (m/z = 18) was separated into three well-resolved peaks, centered at 195, 575, and 825 °C. The ratio of their areas is approximately 10:5:1 (Figure 1d). This result confirms that thermal treatment leads to the desired silica surfaces (hydroxylated and hydrophobic, see Figure 1a), and indicates that, for the pristine, untreated silica sample, the amount of adsorbed water (represented by the area of the first MS peak) is roughly equal to the number of the external (surface) hydroxyls (indicated by the area of the second MS peak). In addition, the third peak on the MS profile is attributed to desorption of the internal (structural) silanols, which are unreachable by adsorbate molecules and not involved in any surface reactions.[46] According to the overall TG weight loss (2.2%) and MS profile, we are able to calculate the surface hydroxyl density, which is approximately 2.5 ± 0.1 OH per nm^2, in agreement with that expected from silica surfaces.[48−50]

The water adsorption isotherms at 25 °C and corresponding differential enthalpy ($\Delta h_{ads\text{-}zero}$) are plotted in Figure 2. A type

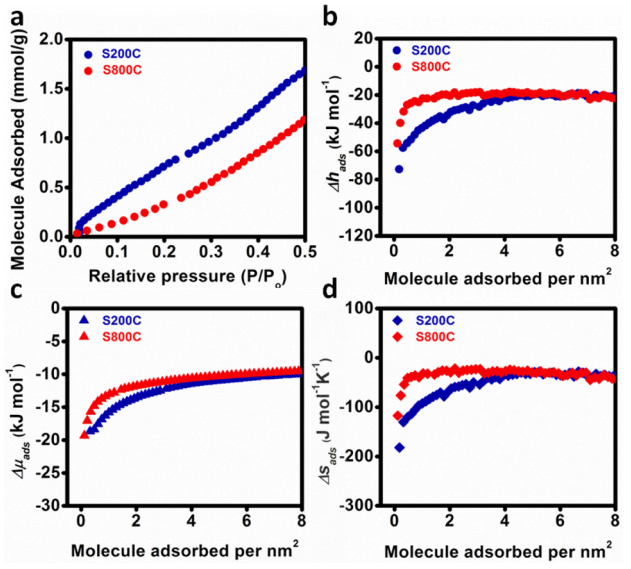

Figure 2. (a) Water adsorption isotherms and (b) corresponding differential enthalpies, (c) free energies, and (d) differential entropies of water adsorption curves at 25 °C on hydroxylated and dehydroxylated (hydrophobic) silica glass sample.

II isotherm is observed for S200C, suggesting favorable water−silica interaction. In contrast, water adsorption on S800C leads to a type III isotherm, indicating that the water−silica surface binding is unfavorable. For S200C, the zero-coverage differential enthalpy of water adsorption ($\Delta h_{ads\text{-}water\text{-}zero}$) is the most exothermic (−72.7 ± 3.1 kJ/mol water). $\Delta h_{ads\text{-}water}$ becomes gradually less exothermic with increasing coverage, until reaching its only plateau (−20.7 ± 2.2 kJ/mol water) at about 5 water molecules per nm^2 (see Figure 2b). On the other hand, for S800C, soon after the adsorption initiates ($\Delta h_{ads\text{-}water\text{-}zero}$ = −54.3 ± 4.5 kJ/mol water), $\Delta h_{ads\text{-}water}$ switches to a plateau (−21.4 ± 4.1 kJ/mol water). Such different behavior strongly suggests that the water−silica interaction is tightly correlated with the presence of surface hydroxyls.

The adsorption energetics of ethanol−silica interactions exhibits different behavior from water (Figure 3). First, nearly

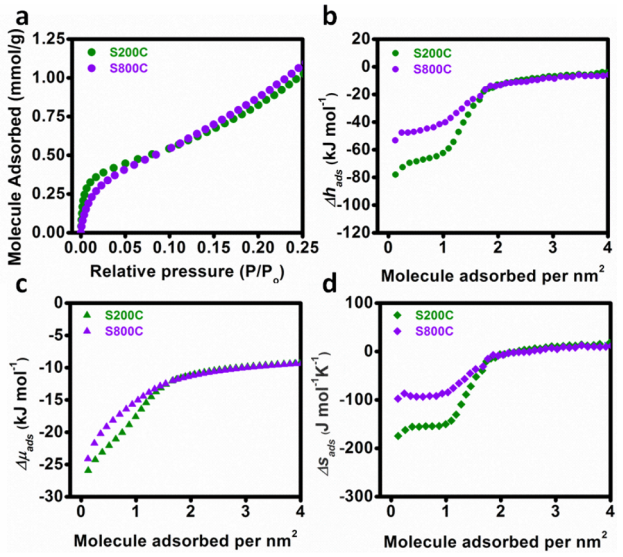

Figure 3. (a) Ethanol adsorption isotherms and (b) corresponding differential enthalpies, (c) free energies, and (d) differential entropies of ethanol adsorption curves at 25 °C on hydroxylated and dehydroxylated (hydrophobic) silica glass sample.

overlapping type II isotherms are obtained for ethanol adsorption on S200C and S800C, which suggests dehydroxylation does not significantly impact the favorable adsorbate−adsorbent interaction or the amount of ethanol adsorbed at a given pressure. Additionally, this similar behavior is also a strong indication that thermal treatment does not change the sample surface area. The zero-coverage enthalpies of ethanol adsorption ($\Delta h_{ads\text{-}ethanol\text{-}zero}$) are −78.0 ± 1.9 and −53.2 ± 3.6 kJ/mol ethanol for S200C and S800C, respectively. The magnitudes of $\Delta h_{ads\text{-}zero}$ for water and ethanol are very similar on the same silica sample. As the coverage increases, both the $\Delta h_{ads\text{-}ethanol}$ profiles appear to be stepwise showing two plateaus (Figure 3b). The first plateau occurs with enthalpies of −66.4 ± 4.8 and −46.1 ± 5.3 kJ/mol ethanol for S200C and S800C, respectively. Then $\Delta h_{ads\text{-}ethanol}$ curves become less negative gradually and end at about 2.0 ethanol per nm^2. Interestingly, it appears that ethanol adsorption on silica does not reach complete monolayer coverage (3.6 ethanol per nm^2) as we have seen for nanocalcite. Moreover, the range (from 0 to 1.0 ethanol per nm^2) of the first plateau is the same for S200C and S800C (Figure 3b), which strongly suggests, the loading of ethanol on silica in that range does not depend on surface silanol concentration. The second plateau of $\Delta h_{ads\text{-}ethanol}$, at about −4.0 kJ/mol ethanol for both samples, is much less exothermic than the condensation enthalpy of ethanol (−42.3 kJ/mol). Such adsorption energetics perhaps suggests weak

DOI: 10.1021/acs.jpcc.5b04271
J. Phys. Chem. C 2015, 119, 15428−15433

physisorption between the ethanol covered silica and subsequently introduced ethanol molecules.

DISCUSSION

The present calorimetric investigation offers quantitative insights on a set of crucial interactions with sensitivity and resolution not provided in previous studies. The detailed thermodynamic data lead to a group of general conclusions for water and ethanol adsorption on silica surface. First, the zero coverage enthalpy of adsorption on the same silica surface appears to be essentially identical for water and ethanol (see Figures 2 and 3). Second, for low coverage, at which the molecule−surface interactions dominate, water selectively binds on silanols, while ethanol shows no preference between silanols and siloxanes. Third, at higher loading, the enthalpy of water adsorption on the hydrated silica surface appears to be continuous, but, in contrast, a clear discontinuity of ethanol adsorption enthalpy on silica surface, leading to stepwise plateaus, is observed. Generally, the overall trends for water/ethanol−silica interactions are quite similar to what we observed earlier for nanocalcite.

Various evidence suggests that water binds silica selectively, with only the surface hydroxyls (silanols, SiOH species) showing strong binding. Infrared spectroscopy by Klier et al.[51] also suggest that the silanols are the dominant active centers for water−silica binding, with, in the initial stage, water and silanol reacting with a 1:1 stoichiometry, in which the silanol is the donor and water the acceptor for hydrogen bond formation. Bakaev and Steele,[52] using molecular dynamics (MD) simulation, suggest that the siloxanes are nonreactive to water Their hypotheses have been supported by FTIR and HREELS (high resolution electron energy loss spectroscopy) experiments conducted by Wendt et al.,[53] who demonstrated that silica synthesized at high temperature, having only Si—O—Si bonds, exhibits no evidence for water−silica surface interaction. These studies suggest that silanol is the only active site for water adsorption on silica. The present calorimetric study provides additional quantitative insights supporting these conclusions by highlighting that cleavage of hydroxyls (silanols) eliminates water−silanol interactions ranging from 0 to approximately 2.5 water molecule per nm^2. Instead, once reaction initiates, water molecules tend to interact with each other and cluster on the purely hydrophobic surface of S800C,[54] supported by the immediate switch to the plateau shown in Figure 2b. Interestingly, regardless of the silanol concentration, upon full coverage, the water clusters on both samples have similar energetic states, indicated by the overlapping plateaus on the $\Delta h_{\text{ads-water}}$ curves. In the present experimental conditions, these clusters appear to be roughly 20 kJ/mol less stable in energy than bulk water.

The present thermodynamic analysis is consistent with the conclusions from past studies that ethanol is adsorbed nonselectively on both hydroxyls and the oxygens of Si—O—Si atoms. Using FTIR, Matsumura et al.[55] revealed that the Si—O—Si oxygen bridges could serve as adsorption sites in ethanol hydrogenation on fully dehydroxylated silica (pretreated at 727 °C). Similar phenomena were observed in the study by Natal-Santiago et al.,[56] in which they also attempted to measure the heat of ethanol adsorption on a partially hydroxylated fumed silica using microcalorimetry. Their results showed that the initial heat of adsorption was roughly −100 kJ/mol ethanol. The adsorption heat became less exothermic gradually until reaching a plateau at about −54 kJ/mol ethanol. Notably, the existence of a potential local minimum in an exothermic energy in the heat of ethanol adsorption at about 0.32 mmol/g (∼1.0 ethanol per nm^2) was pointed out, after which the lateral hydrogen bonding between neighboring ethanol molecules started to impact the adsorbate−surface interactions. Interestingly, such local minimum points were observed at the same location on both isotherms and differential enthalpy ($\Delta h_{\text{ads-ethanol}}$) curves for hydroxylated and hydrophobic silicas in the present study. This is strong evidence demonstrating that for ethanol−silica interaction, the ethanol−ethanol hydrogen bonding is significant even before monolayer formation. Such behavior is different from that in ethanol−calcite. We also demonstrate that elimination of surface hydroxyls does not decrease the number of ethanol adsorption sites. Instead, it only weakens the ethanol−silica interactions since the stronger adsorption sites (silanols) are replaced by the Si—O—Si oxygen bridges, which feature weaker affinity. The energetic differences between these two types of interactions are mirrored by the elevated $\Delta h_{\text{ads-ethanol}}$ profile shown in Figure 3b. The number and distribution of such species, spread over a variety of ring sizes, has not been quantified, although a nuclear magnetic resonance study might be useful future work.

The partial molar free energy (chemical potential) and entropy change ($\Delta\mu$ and Δs) plots were also derived for both water and ethanol adsorption on silica (see Figures 2 and 3). Pure water or ethanol vapor phase at 1 atm and 25 °C was defined as the standard state. The partial molar free energy ($\Delta\mu$) was calculated from the isotherm ($\Delta\mu = RT \ln(p/p_o)$, p_o = 1 atm). The equation $\Delta\mu = \Delta h - T\Delta s$ was used to derive Δs. For the same silica sample, both $\Delta\mu$ and Δs tend to become less negative as adsorption proceeds, reflecting fading surface energetic affinity and increasing degree of randomness, respectively. The change of Δs and $\Delta\mu$ mirrors the trend of Δh, appearing to be continuous for water−silica binding, but stepwise for ethanol−silica interactions (Figures 2 and 3).

The fundamental thermodynamic insights presented here highlight the crucial role of the competition of organic sorption and hydration at molecule−material interfaces, especially, when the organics and water are both present in an aqueous liquid phase. Our calorimetric study emphasizes that such competition is very likely to be thermodynamically driven, and closely related to the properties of material surfaces (hydrophobicity and acidity/basicity) and to the chemical functionality of the adsorbate molecules. Water and ethanol are clearly energetically competitive, with overall energetics similar at low concentration but different at higher concentration. In a more general context, the competing binding between water and organics may be tailored at the nanoscale to engineer highly specified technological and medical processes. For instance, the degree of hydration of a catalyst is almost always critical to achieve successful heterogeneous catalytic reactions involving organic compounds and inorganic nanomaterials, such as titania, alumina, silica, and silicate or aluminosilicate zeolites. In the medical context, silica nanoparticles containing biologically active organic molecules are designed for targeted drug delivery in the largely aqueous cellular environment.[57−59] Furthermore, for geochemistry and environmental science, knowing the binding energetics of water and small organics on simple lab-scale inorganic materials with controlled properties may provide models for water−(bio)organic competition on much more complex mineral surfaces. Such thermodynamic insights may enhance our understanding of processes such as CO_2

DOI: 10.1021/acs.jpcc.5b04271
J. Phys. Chem. C 2015, 119, 15428−15433

sequestration through carbonate precipitation, transport of nutrients and pollutants, and oil and gas recovery.

CONCLUSIONS

We investigate the interactions of ethanol and water with silica surface using direct gas adsorption calorimetry. Strong initial binding of adsorbates is observed, in which water may only bind with silanol, while ethanol may bond both silanol and the siloxane. The clustering of water and coating of ethanol on silica surfaces are strongly supported by the thermochemical data. Such phenomena are similar to those in the water/ethanol–nanocalcite system. Knowing the fundamental information on such simple small molecule–material interactions at the organic/inorganic interfaces is very important for further understanding of much more complex systems encountered in technological, medical, environmental, and geological conditions.

AUTHOR INFORMATION

Corresponding Author

*E-mail: anavrotsky@ucdavis.edu.

Notes

The authors declare no competing financial interest.

ACKNOWLEDGMENTS

The calorimetric work was supported by the U.S. Department of Energy, Office of Basic Energy Sciences, Grant DE-FG02-97ER14749. The authors thank Bruce C. Gates for invaluable discussion during Di Wu's Ph.D. exit seminar, which initiated this study. We also thank Krasen Kovachev and Sergey V. Ushakov for instrumental support.

REFERENCES

(1) Treguer, P. J.; De La Rocha, C. L. *Ann. Rev. Mar. Sci.* **2013**, *5*, 477.
(2) Shintaku, H.; Nakajima, K.; Kitano, M.; Ichikuni, N.; Hara, M. *ACS Catal.* **2014**, *4*, 1198.
(3) Lehman, S. E.; Larsen, S. C. *Environ.-Sci. Nano* **2014**, *1*, 200.
(4) Taguchi, A.; Schuth, F. *Microporous Mesoporous Mater.* **2005**, *77*, 1.
(5) Engstrom, K.; Johnston, E. V.; Verho, O.; Gustafson, K. P. J.; Shakeri, M.; Tai, C. W.; Backvall, J. E. *Angew. Chem. Int. Ed.* **2013**, *52*, 14006.
(6) Yue, Q.; Wang, M. H.; Wei, J.; Deng, Y. H.; Liu, T. Y.; Che, R. C.; Tu, B.; Zhao, D. Y. *Angew. Chem. Int. Ed.* **2012**, *51*, 10368.
(7) McKittrick, M. W.; Jones, C. W. *J. Am. Chem. Soc.* **2004**, *126*, 3052.
(8) Mullner, M.; Yuan, J. Y.; Weiss, S.; Walther, A.; Fortsch, M.; Drechsler, M.; Muller, A. H. E. *J. Am. Chem. Soc.* **2010**, *132*, 16587.
(9) Yuan, J. Y.; Xu, Y. Y.; Walther, A.; Bolisetty, S.; Schumacher, M.; Schmalz, H.; Ballauff, M.; Muller, A. H. E. *Nat. Mater.* **2008**, *7*, 718.
(10) Wang, L.; Zhao, W. J.; Tan, W. H. *Nano Res.* **2008**, *1*, 99.
(11) Slowing, I. I.; Trewyn, B. G.; Giri, S.; Lin, V. S. Y. *Adv. Funct Mater.* **2007**, *17*, 1225.
(12) Balas, F.; Manzano, M.; Horcajada, P.; Vallet-Regi, M. *J. Am. Chem. Soc.* **2006**, *128*, 8116.
(13) Seewald, J. S. *Nature* **2003**, *426*, 327.
(14) Stoffyn-Egli, P.; Lee, K. *Spill Sci. Technol. Bull.* **2002**, *8*, 31.
(15) Smith, J. V.; Arnold, F. P., Jr.; Parsons, I.; Lee, M. R. *Proc. Natl. Acad. Sci. U. S. A.* **1999**, *96*, 3479.
(16) Huang, Z. H.; Yao, Y.; Han, L.; Che, S. N. *Chem.—Eur. J.* **2014**, *20*, 17068.
(17) Wallace, A. F.; DeYoreo, J. J.; Dove, P. M. *J. Am. Chem. Soc.* **2009**, *131*, 5244.
(18) Kroger, N.; Deutzmann, R.; Sumper, M. *Science* **1999**, *286*, 1129.
(19) Parida, S. K.; Dash, S.; Patel, S.; Mishra, B. K. *Adv. Colloid Interfac* **2006**, *121*, 77.
(20) Wu, D.; Navrotsky, A. *Geochim. Cosmochim. Acta* **2013**, *109*, 38.
(21) Wangchareansak, T.; Craig, V. S. J.; Notley, S. M. *Langmuir* **2013**, *29*, 14748.
(22) Kirkpatrick, R. J.; Kalinichev, A. G.; Wang, J. *Mineral. Mag.* **2005**, *69*, 289.
(23) Schulz, J. C.; Warr, G. G. *Langmuir* **2002**, *18*, 3191.
(24) Rosso, K. M. *Mol. Model. Theory: Appl. Geosci.* **2001**, *42*, 199.
(25) Hochella, M. F. *Rev. Mineral.* **1990**, *23*, 87.
(26) Shih, Y. H.; Wu, S. C. *Environ. Toxicol. Chem.* **2005**, *24*, 2827.
(27) Rao, M. A.; Violante, A.; Gianfreda, L. *Soil Biol. Biochem.* **2000**, *32*, 1007.
(28) Piccione, P. M.; Laberty, C.; Yang, S. Y.; Camblor, M. A.; Navrotsky, A.; Davis, M. E. *J. Phys. Chem. B* **2000**, *104*, 10001.
(29) Trofymluk, O.; Levchenko, A. A.; Navrotsky, A. *Microporous Mesoporous Mater.* **2012**, *149*, 119.
(30) Navrotsky, A.; Trofymluk, O.; Levchenko, A. A. *Chem. Rev.* **2009**, *109*, 3885.
(31) Wu, D.; Hwang, S. J.; Zones, S. I.; Navrotsky, A. *Proc. Natl. Acad. Sci. U. S. A.* **2014**, *111*, 1720.
(32) Ushakov, S. V.; Navrotsky, A. *Appl. Phys. Lett.* **2005**, 87.
(33) Birkner, N.; Nayeri, S.; Pashaei, B.; Najafpour, M. M.; Casey, W. H.; Navrotsky, A. *Proc. Natl. Acad. Sci. U. S. A.* **2013**, *110*, 8801.
(34) Birkner, N.; Navrotsky, A. *Proc. Natl. Acad. Sci. U. S. A.* **2014**, *111*, 6209.
(35) Navrotsky, A.; Ma, C. C.; Lilova, K.; Birkner, N. *Science* **2010**, *330*, 199.
(36) Navrotsky, A.; Mazeina, L.; Majzlan, J. *Science* **2008**, *319*, 1635.
(37) Tavakoli, A. H.; Maram, P. S.; Widgeon, S. J.; Rufner, J.; van Benthem, K.; Ushakov, S.; Sen, S.; Navrotsky, A. *J. Phys. Chem. C* **2013**, *117*, 17123.
(38) Zhang, P.; Xu, F.; Navrotsky, A.; Lee, J. S.; Kim, S. T.; Liu, J. *Chem. Mater.* **2007**, *19*, 5687.
(39) Gouvea, D.; Ushakov, S. V.; Navrotsky, A. *Langmuir* **2014**, *30*, 9091.
(40) Levchenko, A. A.; Li, G. S.; Boerio-Goates, J.; Woodfield, B. F.; Navrotsky, A. *Chem. Mater.* **2006**, *18*, 6324.
(41) Wu, D.; Gassensmith, J. J.; Gouvea, D.; Ushakov, S.; Stoddart, J. F.; Navrotsky, A. *J. Am. Chem. Soc.* **2013**, *135*, 6790.
(42) Wu, D.; McDonald, T. M.; Quan, Z.; Ushakov, S. V.; Zhang, P.; Long, J. R.; Navrotsky, A. *J. Mater. Chem. A* **2015**, *3*, 4248.
(43) Wu, D. a. N. A. *Proc. Natl. Acad. Sci. U. S. A.* **2015**, *112*, 5314.
(44) Sand, K. K.; Yang, M.; Makovicky, E.; Cooke, D. J.; Hassenkam, T.; Bechgaard, K.; Stipp, S. L. S. *Langmuir* **2010**, *26*, 15239.
(45) Cooke, D. J.; Gray, R. J.; Sand, K. K.; Stipp, S. L. S.; Elliott, J. A. *Langmuir* **2010**, *26*, 14520.
(46) Peng, L.; Qisui, W.; Xi, L.; Chaocan, Z. *Colloids Surf. A* **2009**, *334*, 112.
(47) Barrett, E. P.; Joyner, L. G.; Halenda, P. P. *J. Am. Chem. Soc.* **1951**, *73*, 373.
(48) Mueller, R.; Kammler, H. K.; Wegner, K.; Pratsinis, S. E. *Langmuir* **2003**, *19*, 160.
(49) Rimola, A.; Costa, D.; Sodupe, M.; Lambert, J. F.; Ugliengo, P. *Chem. Rev.* **2013**, *113*, 4216.
(50) Zhuravlev, L. T. *Colloids Surf. A* **2000**, *173*, 1.
(51) Klier, K.; Shen, J. H.; Zettlemo, Ac. *J. Phys. Chem.* **1973**, *77*, 1458.
(52) Bakaev, V. A.; Steele, W. A. *J. Chem. Phys.* **1999**, *111*, 9803.
(53) Wendt, S.; Frerichs, M.; Wei, T.; Chen, M. S.; Kempter, V.; Goodman, D. W. *Surf. Sci.* **2004**, *565*, 107.
(54) Ma, Y. C.; Foster, A. S.; Nieminen, R. M. *J. Chem. Phys.* **2005**, 122.
(55) Matsumura, Y.; Hashimoto, K.; Yoshida, S. *J. Catal.* **1989**, *117*, 135.
(56) Natal-Santiago, M. A.; Dumesic, J. A. *J. Catal.* **1998**, *175*, 252.

DOI: 10.1021/acs.jpcc.5b04271
J. Phys. Chem. C 2015, 119, 15428–15433

(57) Argyo, C.; Weiss, V.; Brauchle, C.; Bein, T. *Chem. Mater.* **2014**, *26*, 435.
(58) Barbe, C.; Bartlett, J.; Kong, L. G.; Finnie, K.; Lin, H. Q.; Larkin, M.; Calleja, S.; Bush, A.; Calleja, G. *Adv. Mater.* **2004**, *16*, 1959.
(59) Slowing, I. I.; Vivero-Escoto, J. L.; Wu, C. W.; Lin, V. S. Y. *Adv. Drug Delivery Rev.* **2008**, *60*, 1278.

DOI: 10.1021/acs.jpcc.5b04271
J. Phys. Chem. C 2015, 119, 15428−15433